

Protonation States of the Chromophore of Denatured Green Fluorescent Proteins Predicted by ab Initio Calculations

Jamal El Yazal,[†] Franklyn G. Prendergast,^{†,‡} David Elliot Shaw,[§] and Yuan-Ping Pang^{*,†,‡,‡,‡}

Contribution from the Mayo Clinic Cancer Center, Tumor Biology Program, Department of Molecular Pharmacology and Experimental Therapeutics, Molecular Neuroscience Program, Mayo Foundation for Medical Education and Research, 200 First Street SW, Rochester, Minnesota 55905, and D.E. Shaw & Co., Inc., 120 West 45th Street, 39th Floor, New York, New York 10036

Received March 10, 2000. Revised Manuscript Received August 1, 2000

Abstract: Green fluorescent proteins (GFPs) are being intensively investigated due to both their unusual optical spectroscopic characteristics and the extraordinary utility of GFPs as tools in biochemistry, cell biology, and molecular genetics. Recent studies have suggested that the spectrophotometric and fluorescence characteristics of GFPs are controlled through protonation states of the GFP chromophore (*p*-hydroxybenzylideneimidazolinone). However, of three protonation sites in the chromophore, only two have been studied. To understand the structural origin of the observed spectrophotometric and fluorescence characteristics of GFPs, employing ab initio methods, we have investigated all the possible protonation sites of the chromophore of denatured GFPs under different pH conditions. Our results suggest that the denatured GFP chromophore exists in not just two protonation states, as widely assumed in the literature, but in five different protonation states that depend on pH over the range -3.2 to 9.4 as assessed from the predicted pK_a values and the self-consistent reaction field continuum calculations of solvation employing Schrödinger's Jaguar 3.5 program. The unexpected complexity of the protonation states of the denatured GFP chromophore postulated here may provide a useful starting point for a further investigation of the protonation states of the intact GFP chromophore responsible for the experimentally observed UV absorption and fluorescence emission properties of structurally intact GFPs.

Introduction

The photophysical properties of green fluorescent proteins (GFPs) are being intensively investigated. This measure of interest is driven not only by the unusual optical spectroscopic characteristics of GFPs themselves, but also by the extraordinary uses of GFPs as genetically encoded markers and as noninvasive intracellular pH sensors in molecular genetics, biochemistry, and cell biology.^{1–6} There is great interest in the structure-based design of mutant GFPs having different spectral properties, an undertaking that might be expected to benefit from a fuller understanding of the physicochemical principles underlying the optical properties of the GFP chromophore.

Available evidence supports the autocatalytic formation of a chromophore, *p*-hydroxybenzylideneimidazolinone, during the folding of some GFPs, such as those found in the bioluminescent coelenterates *Aequorea victoria*⁷ and *Renilla reniformis*⁸ via a

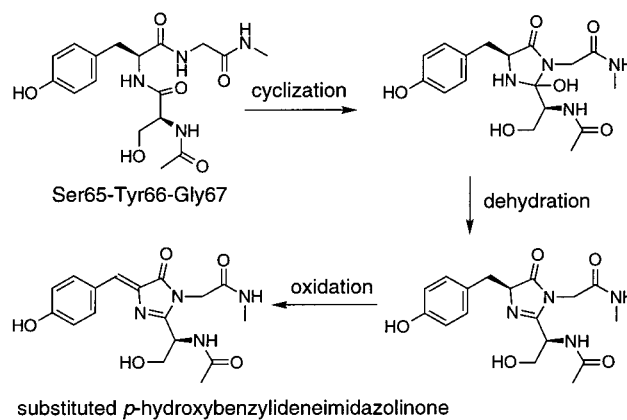


Figure 1. A plausible mechanism for biosynthesis of the GFP chromophore.

mechanism outlined in Figure 1.^{9–11} The chromophore of the denatured wild-type GFPs absorbs maximally at 384 nm at neutral or acidic pH and at 448 nm at alkaline pH,¹² but is totally nonfluorescent under these solution conditions. In contrast, the chromophore of the intact wild-type GFPs absorbs maximally at 395–397 and 475–477 nm, and is intensely fluorescent.^{10,13–15}

* To whom correspondence should be addressed. E-mail: pang@mayo.edu.

[†] Department of Molecular Pharmacology and Experimental Therapeutics, Mayo Foundation for Medical Education and Research.

[‡] Mayo Clinic Cancer Center and Tumor Biology Program, Mayo Foundation for Medical Education and Research.

[§] D.E. Shaw & Co.

[‡] Molecular Neuroscience Program, Mayo Foundation for Medical Education and Research.

(1) Misteli, T.; Spector, D. L. *Nat. Biotechnol.* **1997**, *15*, 961.

(2) Tsien, R. Y. *Annu. Rev. Biochem.* **1998**, *67*, 509.

(3) Prendergast, F. G. *Methods Cell Biol.* **1999**, *58*, 1.

(4) Elsliger, M. A.; Wachter, R. M.; Hanson, G. T.; Kallio, K.; Remington, S. J. *Biochemistry* **1999**, *38*, 5296.

(5) Kneen, M.; Farinas, J.; Li, Y. X.; Verkman, A. S. *Biophys. J.* **1998**, *74*, 1591.

(6) Robey, R. B. et al. *Biochemistry* **1998**, *37*, 9894.

(7) Shimomura, O.; Johnson, F. H.; Saiga, Y. *J. Cell. Comput. Physiol.* **1962**, *59*, 223.

(8) Morin, J. G.; Hastings, J. W. *J. Cell. Physiol.* **1971**, *77*, 313.

(9) Heim, R.; Prasher, D. C.; Tsien, R. Y. *Proc. Natl. Acad. Sci. U.S.A.* **1994**, *91*, 12501.

(10) Cubitt, A. B. et al. *Trends Biochem. Sci.* **1995**, *20*, 448.

(11) Niwa, H. et al. *Proc. Natl. Acad. Sci. U.S.A.* **1996**, *93*, 13617.

(12) Ward, W. W.; Cody, C. W.; Hart, R. C.; Cormier, M. J. *Photochem. Photobiol.* **1980**, *31*, 611.

(13) Cody, C. W.; Prasher, D. C.; Westler, W. M.; Prendergast, F. G.; Ward, W. W. *Biochemistry* **1993**, *32*, 1212.

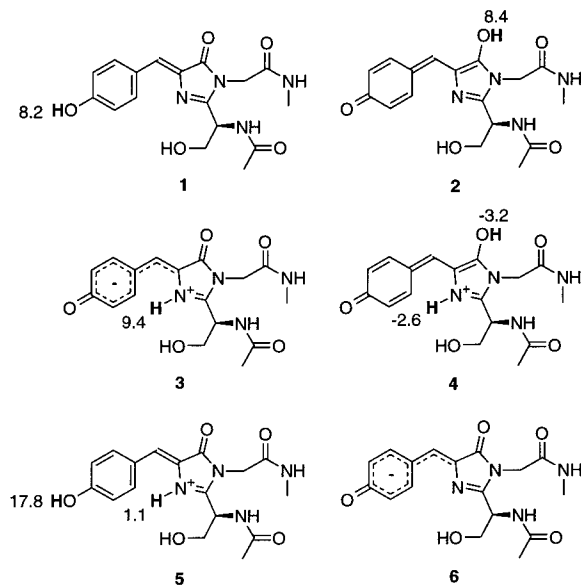


Figure 2. Different protonation states of the substituted GFP chromophore (1–6).

An essential role of proton transfer, tautomerism, in modulating the spectral properties of the chromophore has been inferred from a variety of experimental and theoretical studies.^{2–4,15–18} From the chemical standpoint, the chromophore of GFPs has three protonation sites and possibly six protonation states (1–6, Figure 2). Two protonation states obtained by protonating the carbonyl oxygen atom of imidazolinone in 1 and 5, respectively, which were proposed in the literature,¹⁹ were excluded in our study because of their chemical instability. So far, only the protonation sites at the phenolic oxygen atom and the imidazolinone nitrogen atom of the chromophore have been theoretically and experimentally studied for their relative acidity (pK_a).^{4,16,18,19}

Recently, the electron density maps of *Aequorea* GFP S65T mutant at pH 8.0 and 4.6 have been interpreted as the mutant structures containing the chromophore in the deprotonated and protonated phenolic forms, respectively.⁴ Examining the crystal structure and the electron density map of the mutant at pH 8.0 (PDB codes: 1EMG with resolution of 2.00 Å),⁴ we found that the electron density map could be interpreted as the mutant structure containing the chromophore either in the protonated form or in the deprotonated phenolic form (Figure 3). Considering the electrostatic interactions between Ser205 and Glu222 (Figure 3) and the pK_a of 10.0 for phenol,²⁰ the protonated phenolic form is more likely than the deprotonated phenolic form for the chromophore in the intact mutant at pH 8.0. It is thus not clear that the electron density map of the S65T mutant at pH 8.0 provides experimental evidence for the deprotonated phenolic form of the chromophore. For the same reason, it is also not clear that other X-ray structures of GFPs solved to date provide experimental evidence for the absence of the chro-

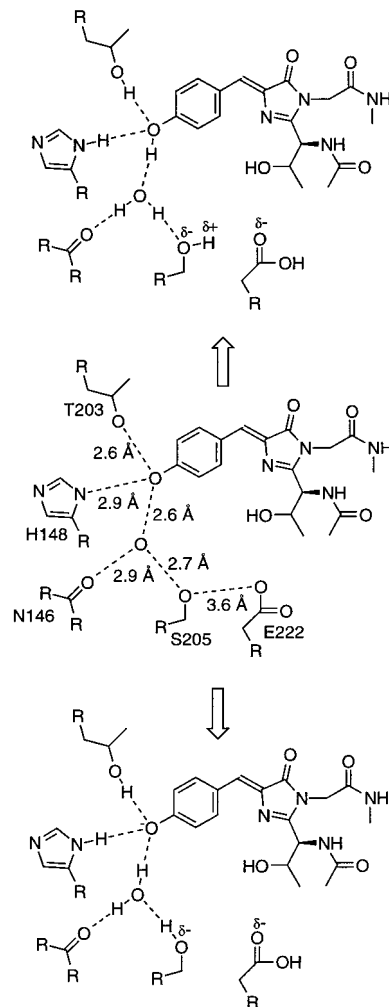


Figure 3. Schematic diagram showing two possible protonation states of the chromophore in the X-ray structure (1EMG) of a GFP mutant at pH 8.0. (The dash line indicates a hydrogen bond.)

mophore with the ring nitrogen atom protonated in the intact GFPs.^{18,21} Although the reported X-ray structures of GFPs offer valuable insight into the relationship between protein structure and spectroscopic function, in our opinion, these structures are not sufficient to deduce the protonation states of the GFP chromophore that are responsible for UV absorption and fluorescence emission.

Accordingly, we chose first to investigate the protonation states of the chromophore in denatured GFPs. The rationale for this decision was that exposure of the denatured GFP chromophore to bulk solvent should allow theoretical prediction of the pK_a value for each protonation site of the chromophore with relatively high accuracy using the continuum dielectric method-based pK_a predictor module of Schrödinger's Jaguar 3.5 program (see Methods). We could then use the calculated pK_a values to predict the protonation states of the denatured GFP chromophore under different pH conditions. If we were able to match the experimentally determined spectra of denatured GFPs with those calculated, we could move more confidently toward rationalizing the spectral properties of intact GFPs.

We report here the theoretical pK_a values for all possible protonation sites of the chromophore in denatured GFPs, the predicted protonation states of the chromophore under different pH conditions, and their biological implications.

(14) Prasher, D. C.; Eckenrode, V. K.; Ward, W. W.; Prendergast, F. G.; Cormier, M. J. *Gene* **1992**, *111*, 229.

(15) Chatteraj, M.; King, B. A.; Bublit, G. U.; Boxer, S. G. *Proc. Natl. Acad. Sci. U.S.A.* **1996**, *93*, 8362.

(16) Voityuk, A. A.; Michelbeyerle, M. E.; Rosch, N. *Chem. Phys. Lett.* **1997**, *272*, 162.

(17) Lossau, H. et al. *Chem. Phys.* **1996**, *213*, 1.

(18) Scharnagl, C.; Raupp-Kossmann, R.; Fischer, S. F. *Biophys. J.* **1999**, *77*, 1839.

(19) Voityuk, A. A.; Michelbeyerle, M. E.; Rosch, N. *Chem. Phys.* **1998**, *231*, 13.

(20) Lange, N. A. *Handbook of Chemistry*; McGraw-Hill: New York, 1979.

(21) Wachter, R. M.; Elslinger, M. A.; Kallio, K.; Hanson, G. T.; Remington, S. J. *Structure* **1998**, *6*, 1267.

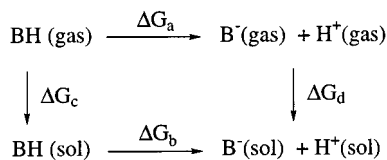


Figure 4. A closed thermodynamic cycle used in pK_a calculations.

Methods

The structures of the substituted *p*-hydroxybenzylideneimidazolinone shown in Figure 2 were taken from the X-ray structure of *Aequorea* GFP (PDB code: 1EMC)²² and energy minimized with the Quanta program using the CHARMM force field.²³ The molecular mechanically optimized structures were then used as starting structures for the Schrödinger pK_a prediction module²⁴ implemented in the Jaguar 3.5 program.²⁵ Because the relative stabilities of the *p*-hydroxybenzylideneimidazolinone structures in different configurational states had not been reported, we optimized the *p*-hydroxybenzylideneimidazolinone structures in the cationic, neutral, zwitterionic, and anionic forms in both singlet and triplet states with the B3LYP/6-311+G(d,p) method. We found that the singlet state structures in all four protonation forms were at least 27 kcal/mol more stable than those in the triplet state. Such energy differences are significant according to the chemical accuracy of 2 kcal/mol.²⁶ Therefore, only structures in the singlet state shown in Figure 2 were used in the pK_a calculations. The harmonic frequencies used to preclude the low-energy transition-state conformations of the substituted chromophore structures in different protonation states were calculated using the HF/6-31G//HF/6-31G method.

The pK_a prediction module computes a raw pK_a value of a structure BH according to eqs 1–4 that are derived from a closed thermodynamic cycle shown in Figure 4 according to the reported continuum dielectric method,²⁷ where $E_{X(\text{gas})}$ is obtained from an ab initio calculation with the B3LYP/cc-pVTZ(-f)[+]/B3LYP/6-31G[**] (the functions in brackets are applied to the atoms involved in deprotonation.) method;^{28–30} ΔG_{sol_X} is derived from a self-consistent reaction field continuum calculation of solvation³¹ using the B3LYP/6-31[+]/B3LYP/6-31G[**] (the functions in brackets are applied to the atoms involved in deprotonation.) method; $\Delta G_{\text{sol}_{\text{H}^+}}$ is directly taken from the experimental value of -259.5 kcal/mol;³² and $T\Delta S$ is approximated by the reported entropy of a proton ($T\Delta S = 7.8$ kcal/mol).²⁷ A predicted pK_a value is then obtained from the raw pK_a value with an empirical correction according to eq 5.

$$pK_a(\text{raw}) = \Delta G_b/2.3RT = (\Delta G_a + \Delta G_d - \Delta G_c)/2.3RT \quad (1)$$

$$\Delta G_a = \Delta H - T\Delta S = E_{\text{B}^{\ominus}(\text{gas})} - E_{\text{BH}(\text{gas})} + (\delta/2)RT - T\Delta S \quad (2)$$

$$\Delta G_d = \Delta G_{\text{sol}_{\text{B}^{\ominus}}} + \Delta G_{\text{sol}_{\text{H}^+}} \quad (3)$$

$$\Delta G_c = \Delta G_{\text{sol}_{\text{BH}}} \quad (4)$$

$$pK_a = A * pK_a(\text{raw}) + B \quad (5)$$

Several features of Schrödinger's method that distinguish it from purely empirical fragment-based approaches are described as follows. First, the use of ab initio calculations rather than fragment table lookups and interpolation will lead to a substantially wider range of applicability.

(22) Palm, G. J. et al. *Nat. Struct. Biol.* **1997**, *4*, 361.

(23) QUANTA/CHARMM San Diego, CA, 1997.

(24) Klicic, J. J.; Perry, J. K.; Ringnalda, M. N. *ACS Meeting Abstr. 215, Part 1* **1998**, 127.

(25) JAGUAR 3.5; 1998 ed.; Shrodinger, Inc.: Portland, OR, 1998.

(26) Remko, M.; Liedl, K. R.; Rode, B. M. *J. Phys. Chem.* **1998**, *102*, 771.

(27) Lim, C.; Bashford, D.; Karplus, M. *J. Phys. Chem.* **1991**, *95*, 5610.

(28) Woon, D. E.; Dunning, T. H. *J. Chem. Phys.* **1993**, *98*, 1358.

(29) Dunning, T. H., Jr. *J. Chem. Phys.* **1989**, *90*, 1007.

(30) Kendall, R. A.; Dunning, T. H. J.; Harrison, R. J. *J. Chem. Phys.* **1992**, *96*, 6796.

(31) Marten, B. et al. *J. Phys. Chem.* **1996**, *100*, 11775.

(32) Reiss, H.; Heller, A. *J. Phys. Chem.* **1985**, *89*, 4207.

Table 1. A Summary of the pK_a Predictions for Different Classes of Molecules Including the Number of Cases and Average Deviations from the Experimental Values^a

type of molecule	no. of molecules	mean abs dev
carboxylic acid	40	0.7
alcohol	16	1.2
hydroxamic acid	14	0.4
phenol	9	0.1
thiol	5	0.6
aniline	5	0.2
<i>N</i> heterocycle	16	0.3
primary amine	7	0.7
secondary amine	7	0.4
tertiary amine	11	0.5
imides	8	0.8
barbituric acid	5	0.2
tetrazole	6	0.5
amidine	4	0.3
benzodiazepine	5	0.4
pyrrole	4	0.4
indole	4	0.1

^a J. J. Klicic of Schrödinger, Inc., personal communication.

Table 2. Comparisons of the Calculated pK_a Values with the Experimental Values^{20,34,35} of the Chromophore-Related Phenol and Its Analogues^a

molecule	exp	calc.d	dev
4-hydroxybenzaldehyde	7.6	7.7	-0.1
4-chlorophenol	9.4	9.6	0.2
4-fluorophenol	9.9	9.8	-0.1
4-methoxyphenol	10.2	10.5	0.3
4-methylphenol	10.3	10.3	0.04
4-aminophenol	10.5	10.1	-0.4
4-nitrophenol	7.2	7.1	-0.02
<i>p</i> -xylol	10.4	10.5	0.1
phenol	10.0	9.8	-0.1
mean abs dev			0.1

^a J. J. Klicic of Schrödinger, Inc., personal communication.

as well as significantly higher precision when the compound in question has no similar entries in the empirical table. Second, this method allows for a reasonable treatment of conformational effects, which are, in general, entirely missing from fragment-based methods. Last, this method can systematically handle multiple protonation sites of a molecule such as the chromophore shown in Figure 2.

Results and Discussion

Control Studies. The reliability and accuracy of the pK_a predictor are demonstrated by the summary of the pK_a predictions of different classes of molecules and average deviations from the experimental values listed in Table 1, and by the comparison of the predicted pK_a values with the experimental values of the chromophore-related phenol and its analogues listed in Table 2 (personal communication from J. Klicic of Schrödinger, Inc.). The mean absolute deviations from the experimental values range from 0.01 to 1.2 pK_a units (Table 1). These results suggest that the uncertainty of the predicted pK_a values is about 1.2 pK_a units.

Predicted pK_a Values. To best represent the chromophore of denatured GFPs, we used the substituted *p*-hydroxybenzylideneimidazolinone with its *N*- and *C*-termini masked with acetyl and methylamino groups, respectively, as shown in Figure 2. For the three neutral forms of the substituted chromophore, our calculations suggest that the pK_a values of the phenolic form (**1**), the quinonoid form (**2**), and the zwitterionic form (**3**) are 8.2, 8.4, and 9.4, respectively (Figure 2). For the two cationic forms of the substituted chromophore, the predicted pK_a values of the hydroxyl proton of the chromophore in the cationic

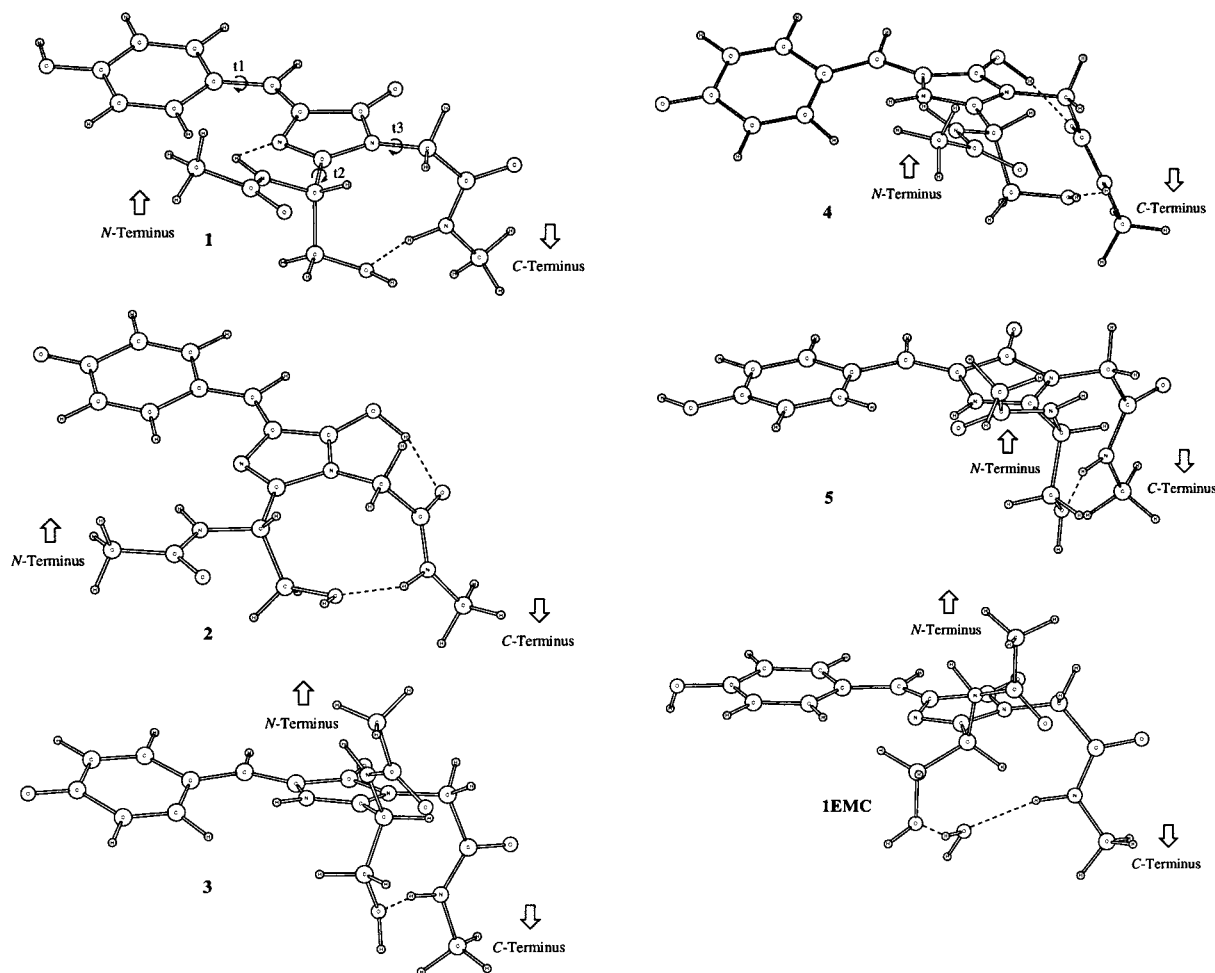


Figure 5. Comparison of all the protonated, quantum mechanically optimized chromophore structures (1–5) with the structure whose heavy atom coordinates were taken from the X-ray structure of the GFP (PDB code: 1EMC) showing that the *N*- and *C*-termini of each structure are located on opposite sides of the imidazolinone plane by a hydrogen bond. (Dash lines indicate hydrogen bonds, and arrows indicate opposite locations of the *N*- and *C*-termini relative to the imidazolinone plane.)

Table 3. Relative Energies (kcal/mol) of the Substituted Chromophore in Different Protonation Forms in Vacuum and in Water Calculated with the Self-Consistent Reaction Field Continuum Model

	1	2	3	4	5
vacuo	-787792	-787779	-787765	-788008	-788035
water	-787630	-787611	-787629	-787929	-787947

quinonoid form (4) and in the cationic phenolic form (5) are -3.2 and 17.8, respectively, while the pK_a values of the nitrogen proton in 4 and in 5 are -2.6 and 1.1, respectively (Figure 2).

Geometry and Relative Stability of the Chromophore Structures. Inspecting the quantum mechanically optimized structures of the substituted chromophore in five different protonated states (1–5) in the gas phase used in our pK_a calculations, we found that the acetyl-masked *N*-terminus of all the optimized chromophore structures is located on one side of the chromophore and the methylamino-masked *C*-terminus of the chromophore is located on the other side, which resembles the chromophore conformation (1EMC shown in Figure 5) identified in the X-ray structure of the GFP (PDB code: 1EMC),²² as indicated by the torsions listed in Table 4. There is a hydrogen bond between the hydroxyl group of the Ser residue and the peptide nitrogen proton in these optimized structures (Figure 5). In the X-ray structure, the corresponding hydrogen bond donor and acceptor is bridged by a water molecule (Figure 5). The hydrogen bond of the Ser hydroxyl

Table 4. Torsions (degree of arc) Calculated from the Chromophore Structures Obtained from ab Initio Calculations and from Crystallographic Analysis (for torsion definitions, see Figure 5)

structure	t_1	t_2	t_3
1	176.6	-88.2	-67.8
2	-179.7	-63.0	-67.0
3	168.9	-117.9	-82.4
4	172.4	-69.2	-62.5
5	-172.7	-111.6	-75.7
1EMC	178.0	-160.7	-90.6

group locks the trans-configuration of the *N*- and *C*-termini in all six conformations shown in Figure 5. The conformational similarity between the chromophore structure optimized in vacuo and the chromophore structure in GFPs (Table 4) suggests that it is reasonable to use the optimized structure in vacuo in the self-consistent reaction field continuum calculations of solvation.

For the neutral forms of the substituted chromophore, the single-point energy calculations with the B3LYP/cc-pVTZ(-f)-[+]/B3LYP/6-31G[**] (the functions in brackets were applied to the atoms involved in deprotonation) method reveal that the phenolic form (1) is 13 and 27 kcal/mol more stable than the quinonoid form (2) and the zwitterionic form (3), respectively, in vacuo (Table 3). Interestingly, the self-consistent reaction field continuum calculations of solvation using the B3LYP/6-31[+]/G**/B3LYP/6-31G[**] (the functions in brackets were

applied to the atoms involved in deprotonation) method suggest that, in water, the phenolic form (**1**) is as stable as the zwitterionic form (**3**), but is 19 kcal/mol more stable than the quinonoid form (**2**) (Table 3). According to the chemical accuracy of 2 kcal/mol,²⁶ these results suggest that the neutral chromophore exists in the phenolic form (**1**) in vacuo, but is in equilibrium between the phenolic (**1**) and zwitterionic (**3**) forms in water. For the cationic forms of the chromophore, the calculations with the same methods reveal that the cationic phenolic form (**5**) is 27 and 18 kcal/mol more stable than the cationic quinonoid form (**4**) in vacuo and in water, respectively (Table 3).

Protonation States of the Chromophore. Our calculations suggest that at pH greater than 9.4 the chromophore of denatured GFPs exists in the anionic form (**6**). A calculation of the absorption spectrum with the ZINDO method³³ revealed that **6** in the presence of explicit water molecules showed absorption at 456 nm with $f = 1.008$ (calculation details to be published separately). These results agree with the report that the guanidine-denatured *Aequorea* GFP at a pH of 10.8 showed absorption at 448 nm.¹² At pH over the range 1.1 to 9.4, our calculations suggest that the chromophore exists mainly in the neutral phenolic form (**1**) and the zwitterionic form (**3**), which are in equilibrium. Calculations of the absorption spectra of **1** and **3** with the ZINDO method showed absorption of **3**, but not **1**, in the presence of explicit water molecules at 398 nm with $f = 0.733$. This result is also in accordance with the report that the guanidine-denatured *Aequorea* GFP at pH of 6.6 had absorption at 384 nm.¹² At pH 8.8 (an average of pK_a of 8.2 from **1** and pK_a of 9.4 from **3**), our calculations suggest that the substituted chromophore exists in the neutral phenolic form (**1**), the zwitterionic form (**3**), and the anionic form (**6**), and it has absorption equally at 355 and 456 nm according to the ZINDO calculations. Indeed, the experimentally observed isosbestic point at 405 nm for the guanidine-denatured *Aequorea* GFP was found at pH of 8.1.¹² The difference between the predicted and experimental pH values for the isosbestic point is only 0.7 pK_a unit, which is within the expected uncertainty of 1.2 pK_a units. At pH over the range -3.2 to 1.1, the chromophore is mainly in the cationic phenolic form (**5**). At pH less than -3.2 , the chromophore is mainly in the cationic quinonoid form (**4**), a protonation state that has not been reported hitherto.¹⁹

Biological Implications. The present work reveals the unexpected complexity of the protonation states of the denatured GFP chromophore. Although the ab initio calculations suggest that the neutral quinonoid form (**2**) is not a populated protonation

form at any pH value, they still predict three different protonation forms at pH over the range 8.2 to 9.4. We thus believe these results call into question the assumption that the originally reported pH of 8.1 for the isosbestic point of the chromophore of the denatured and pronase-digested GFPs¹² is the pK_a of the chromophore.^{2,4,21} On the basis of the intrinsic chemical nature of the GFP chromophore and the data from the present study, it may also be premature to assume the experimentally observed pH for the isosbestic point of the intact GFP chromophore to be the pK_a value for the intact GFP chromophore^{18,21} in the absence of further investigation. The results reported here also suggest that the reported hypothesis¹⁶ that the cationic phenolic form (**5**) in the intact GFP is responsible for the absorption at 397 nm might be worthy of reinvestigation; according to our predicted pK_a , the cationic form exists at a pH of 1.1 or lower, at which point the protein would be denatured unless the protein environment of GFPs greatly increased the pK_a of the ring nitrogen atom of the chromophore.

Conclusions

The present work reveals that the difference between the predicted and experimental pH values for the isosbestic point of the chromophore is only 0.7 pK_a unit, which is within the expected uncertainty of 1.2 pK_a units, and provides evidence of the reliability and accuracy of the Schrödinger pK_a prediction module. Using this pK_a prediction module, our calculations suggest that the chromophore of denatured GFPs exists in five different protonation states at pH over the range -3.2 to 9.4. At pH greater than 9.4, our calculations suggest that the chromophore exists in the anionic form (**6**). At pH over the range 1.1 to 9.4, our calculations suggest that the chromophore exists mainly in the neutral phenolic form (**1**) and the zwitterionic form (**3**) which are in equilibrium. At pH 8.8, our calculations suggest that the chromophore exists in the neutral phenolic form (**1**), the zwitterionic form (**3**), and the anionic form (**6**). Our calculations suggest that the chromophore is mainly in the cationic phenolic form (**5**) at pH over the range -3.2 to 1.1, and mainly in the cationic quinonoid form (**4**) at pH less than -3.2 . The unexpected complexity of the protonation states for the denatured GFP chromophore postulated here may provide a useful starting point for a further investigation of the protonation states of the intact GFP chromophore responsible for the experimentally observed UV absorption and fluorescence emission properties of structurally intact GFPs.

Acknowledgment. This work was supported by the Mayo Foundation for Medical Education and Research, the NIH GM 34847 (F.G.P.), and Attenuon, L.L.C.(Y.P.P.). We thank Dr. J. J. Klicic of Schrödinger, Inc. for providing unpublished data and comments on the manuscript.

JA0008721

(33) Zerner, M. C.; Loew, G. H.; Kirchner, R. R.; Mueller-Westerhof, U. T. *J. Am. Chem. Soc.* **1980**, *102*, 589.

(34) Serjeant, E. P.; Dempsey, B. *Ionisation Constants of Organic Acids in Aqueous Solution*; Pergamon Press: New York, 1979.

(35) Kortum, G.; Vogel, W.; Andrustow, K. *Pure Appl. Chem.* **1961**, *1*.